Int. J. Reliability and Safety, Vol. X, No. Y, XXXX

A Bayesian methodology for crack identification in structures using strain measurements

S. Gaitanaros, G. Karaiskos,
C. Papadimitriou* and N. Aravas

Department of Mechanical and Industrial Engineering,
University of Thessaly,
Pedion Areos,
Volos 38334, Greece
Email: stgaitan@uth.gr Email: gkaraiskos@uth.gr
Email: costasp@uth.gr Email: aravas@uth.gr
*Corresponding author

Abstract: A Bayesian system identification methodology is presented for estimating the crack location, size and orientation in a structure using strain measurements. The Bayesian statistical approach combines information from measured data and analytical or computational models of structural behaviour to predict estimates of the crack characteristics along with the associated uncertainties, taking into account modelling and measurement errors. An optimal sensor location methodology is also proposed to maximise the information that is contained in the measured data for crack identification problems. For this, the most informative, about the condition of the structure, data are obtained by minimising the information entropy measure of the uncertainty in the crack parameter estimates. Both crack identification and optimal sensor location formulations lead to highly non-convex optimisation problems in which multiple local and global optima may exist. A hybrid optimisation method, based on evolutionary strategies and gradient-based techniques, is used to determine the global minima. The effectiveness of the proposed methodologies is illustrated using simulated data from a single crack in a thin plate subjected to static loading.

Keywords: crack identification; Bayesian analysis; information entropy; sensor placement.

Reference to this paper should be made as follows: Gaitanaros, S., Karaiskos, G., Papadimitriou, C. and Aravas, N. (XXXX) 'A Bayesian methodology for crack identification in structures using strain measurements', *Int. J. Reliability and Safety*, Vol. X, No. Y, pp.xxx–xxx.

Biographical notes:[AQ1]

AQ1: Please provide brief career histories (maximum 100 words each) of the following authors:

'S. Gaitanaros', 'G. Karaiskos', 'C. Papadimitriou' and 'N. Aravas'.

1 Introduction

The problem of crack detection in structures has received much attention over the years because of its profound importance in structural health monitoring. Early detection of cracks is a key element for preventing catastrophic failure and prolonging the life of structures. Crack identification information can be used for developing cost-effective maintenance procedures for structures, improving their safety and reducing their maintenance and rehabilitation costs, in a whole-life cost basis. Current inspection techniques involve complex, time-consuming procedures, which can be very labour-intensive and expensive. A fast, low-cost built-in structural health monitoring system involving a sensor array along with fast processing techniques is needed to overcome the shortcomings of the current inspection techniques.

Damage detection is generally approached by several techniques. One category of them is based on the changes in the global vibrational properties of a structure caused by damage (Doebling et al., 1996; Hjelmstad and Shin, 1996; Doebling et al., 1998; Vanik et al., 2000; Ihn and Chang, 2004; Mal et al., 2005). However, this approach is only effective in dealing with larger defects for the obvious reason that the effects of small flaws on the global vibrational properties are often below the noise level in large structures. Other techniques use changes in the characteristics of ultrasonic waves propagating across existing defects (Giurgiutiou et al., 2001; Lee and Staszewski, 2003; Paget et al., 2003). Ultrasonic approaches, although highly effective in detecting very small defects, require a dense network of sensors that is impractical to implement in larger structures and raises significantly the cost of the equipment. Techniques based on strain measurements from optical fibres for identifying cracks have also been pursued numerically, analytically and experimentally (Munns et al., 2002; Tsamasphyros et al., 2003a; Tsamasphyros et al., 2003b). Based on the experimental results (Munns et al., 2002), this method has been shown to be promising for detecting cracks. Limited studies have shown that the method effectiveness depends on the location and number of sensors with respect to the crack. This paper investigates the problem of identifying cracks using an array of strain measurements. It presents analytical methods and computational tools that are required to identify cracks by combining information from strain measurements and computational models of the structure. It also addresses the experimental design problem related to finding the optimal location, orientation, number and density of sensors for reliable detection, along with the computational difficulties involved.

The objective of the present study is twofold. Firstly, a methodology for the estimation of the crack parameters based on a statistical system identification methodology is presented. The crack parameters may include crack location, size and orientation. Their values are estimated using measured data from a structure subjected to static loading. The Bayesian approach to statistical modelling uses probability as a way of quantifying the plausibilities associated with the various models and the values of the parameters of these models given the observed data (Beck and Katafygiotis, 1998; Katafygiotis et al., 1998; Katafygiotis et al., 2000; Christodoulou and Papadimitriou, 2007). Probability distributions are used to quantify the various uncertainties in the values of the crack parameters and these distributions are then updated based on information contained in the measured data. The location and size of damage is inferred from the most probable values of the crack parameters obtained as the ones that maximise the posterior probability distribution of the parameters given the measured data.

Secondly, a formulation for the optimal design of sensor configuration for crack identification is presented based on the information entropy measure. Previous work addressing the issue of optimally locating a given number of sensors in a structure has been carried out by several investigators. In particular, information theory based approaches (e.g. Kammer, 1991; Kirkegaard and Brincker, 1994; Udwadia, 1994; Papadimitriou et al., 2000) have been developed to provide rational solutions to several issues encountered in the problem of selecting the optimal sensor configuration. These approaches are closely correlated with the problem of identification and damage detection using vibrational or modal properties. Herein, the information entropy is used to measure the quality of information that can be extracted from the data used to detect a crack. The optimal strain sensor configuration (position and orientation of strain sensors) is obtained as the one that minimises the information entropy. An important advantage of the information entropy measure is that it allows us to make comparisons between sensor configurations involving a different number of sensors in each configuration (Papadimitriou et al., 2000; Papadimitriou, 2004a). The information entropy is particularly useful for trading-off cost of instrumentation with information gained from additional sensors about the condition of the structure, thus making cost-effective decisions regarding optimal instrumentation.

The presentation in this work is organised as follows. In Section 2, the crack parameter identification methodology is presented for the general case of a cracked structure and strain measurements. In Section 3, a formulation for the design of the optimal sensor configuration for crack identification based on the information entropy measure is presented. Both the crack estimation problem and the optimal sensor configuration problem are formulated as highly non-convex optimisation problems. Section 4 briefly reviews a hybrid optimisation algorithm combining evolutionary and gradient-based algorithms for the estimation of the global optima in both problems of crack identification and optimal sensor location. In Section 5, the effectiveness of the proposed identification methodology and computational algorithms is illustrated for the case of a crack in a thin plate subjected to uniform biaxial tension. The simulated data are generated by a computational mechanics problem simulating the behaviour of a bounded plate with crack, adding noise in the predictions in order to simulate the effect of measurement error. In order to simulate modelling error, the model used to predict the strain field is based on analytical solutions for the strain field available for the case of infinite plate dimensions. In addition, optimal sensor configurations using the proposed computational algorithms are derived and their effectiveness in improving crack detectability is explored. Finally, the conclusions are summarised in Section 6.

2 Bayesian formulation for identifying crack parameters

Consider one or more cracks on a structure subjected to far field static loading (e.g. distributed stress, force, etc.). The objective is to identify the crack locations, sizes and orientations using measured data such as strain measurements. For this, a vector of parameters $\underline{\theta} \in R^{N_\theta}$ defining the crack locations, sizes and orientations is introduced and the problem of crack identification is equivalent to the problem of estimating the value of the parameter set $\underline{\theta}$.

Specifically, consider the case of a single crack of length $2a$ in a bounded plate, shown in Figure 1, subjected to biaxial tension. This plate could model a part of a larger structure as in Figure 2. Let the crack have an orientation of angle ϕ and its centre be located at (x_0, y_0) with respect to a coordinate system. A parameter vector $\underline{\theta}$ that completely defines the crack and is to be identified, involves crack location (x_0, y_0), length $2a$ and orientation ϕ so as $\underline{\theta} = \{x_0, y_0, a, \phi\}$. In the case of unknown loading, far field stresses σ_x, σ_y should be included in $\underline{\theta}$ so that the parameter set is $\underline{\theta} = \{x_0, y_0, a, \phi, \sigma_x, \sigma_y\}$.

Figure 1 Case of a crack of length $2a$ in a plate subjected to biaxial tension

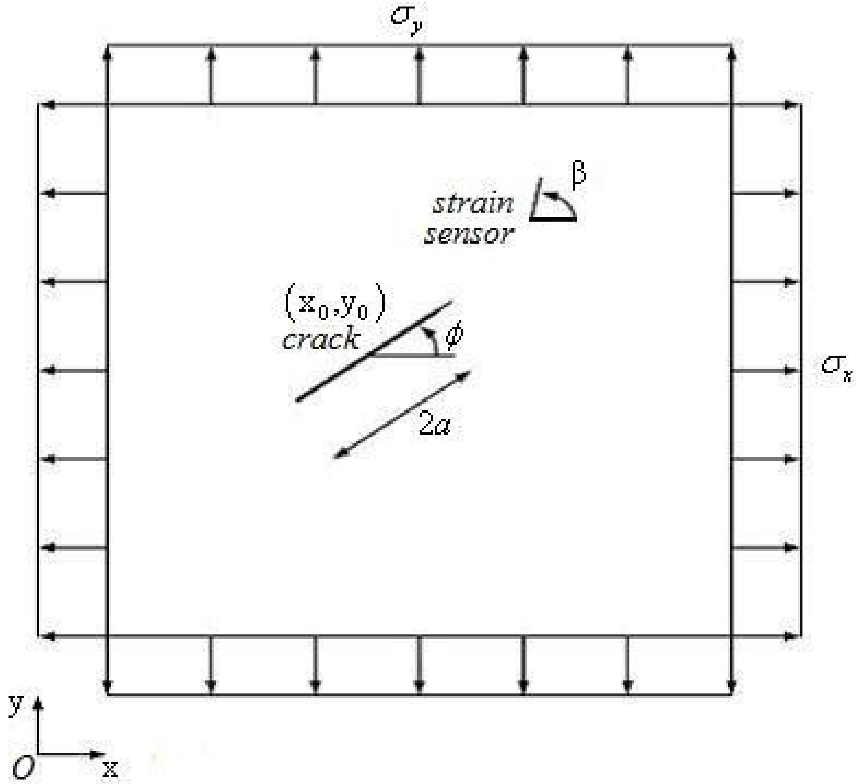

A Bayesian statistical system identification methodology is used to estimate the values of the parameter set $\underline{\theta}$ and their associated uncertainties using the information provided from test data as follows. Let $D = \{\hat{\varepsilon}^{(m)}(\underline{r}_i, \beta_i),\ i = 1,\ldots,N_0, m = 1,\ldots,N\}$ be the measured strain data, where $\underline{r}_i$ is the position vector indicating the location of the ith measurement, β_i is the angle indicating the direction of the ith measurement, N_0 is the number of sensors in a sensor array and N is the number of datasets available from measurements at different time instants. Let $\mathcal{M}$ be a class of models parameterised by the parameter set $\underline{\theta}$, simulating the behaviour of the structure with cracks. Let also

$\varepsilon^{(m)}(\underline{r};\beta;\underline{\theta})$ be the response prediction at location $\underline{r}$ and direction β from a model in the class M corresponding to a particular value of the parameter set $\underline{\theta}$. Herein, the model class is associated with the solution of the stress and strain field model around a crack tip. These solutions can be provided by analytical expressions available for infinite plates or can be given from computational finite element models for bounded plates. Thus, each model class corresponds to different modelling assumptions that can affect the reliability of the methodology for detecting cracks.

Figure 2 Plate as a part of a larger structure

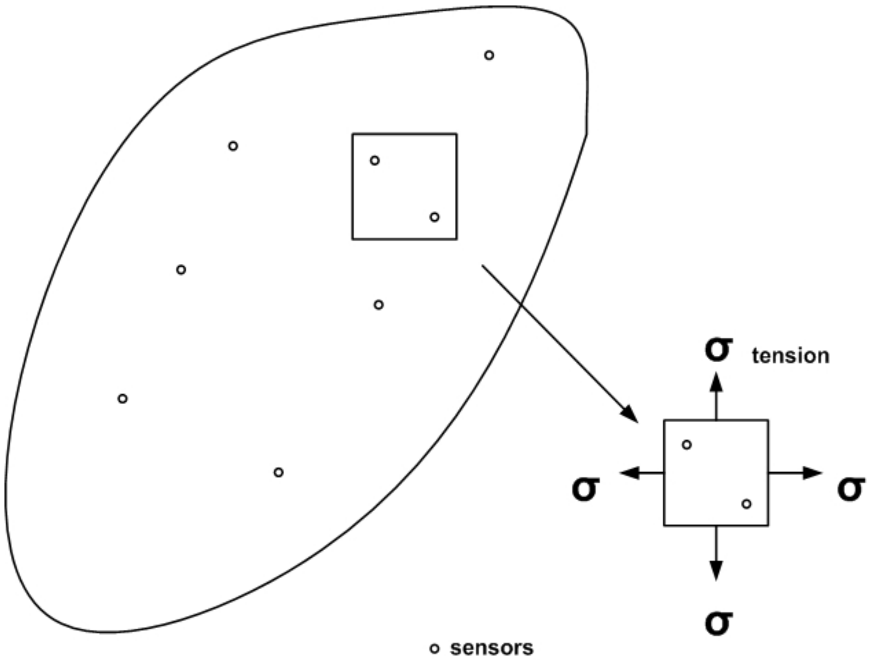

The measured response and the model response predictions satisfy the prediction error equation

$$\hat{\varepsilon}^{(m)}(\underline{r}_i,\beta_i)=\varepsilon^{(m)}(\underline{r}_i,\beta_i;\underline{\theta})+n^{(m)}(\underline{r}_i,\beta_i;\underline{\theta}),\quad i=1,\ldots,N_0,\quad m=1,\ldots,N \tag{1}$$

where $n^{(m)}(\underline{r}_i,\beta_i;\underline{\theta})$ is model prediction error that is due to modelling error and measurement noise. The prediction error in the $\underline{r}_i$ location with orientation β_i is assumed to be a zero-mean Gaussian variable, $n^{(m)}(\underline{r}_i,\beta_i;\underline{\theta})\sim N(0,s_i^2)$, with variance s_i^2.

According to the Bayesian system identification methodology (Beck and Katafygiotis, 1998), the values of crack parameters $\underline{\theta}$ and the prediction error parameters $\underline{s}=(s_1,s_2,\ldots,s_N)$ are modelled by Probability Density Functions (PDF) that quantify the plausibility of each possible value of the crack parameter set $\underline{\theta}$ and prediction error parameter set $\underline{s}$. Applying the Bayes' theorem and assuming independence of the prediction errors, the updating posterior PDF $p(\underline{\theta}, \underline{s} \mid D)$ of the set of parameters $(\underline{\theta}, \underline{s})$ given the measured data D takes the form (Christodoulou and Papadimitriou, 2007):

$$p(\underline{\theta}, \underline{s} \mid D) = \frac{c_1}{\left(\sqrt{2\pi}\right)^{N_0 N} \rho(\underline{s})} \exp\left[-\frac{N_0 N}{2} J(\underline{\theta}; \underline{s})\right] \pi(\underline{\theta}, \underline{s}) \tag{2}$$

where

$$J(\underline{\theta}, \underline{s}; D) = \frac{1}{N_0} \sum_{i=1}^{N_0} \frac{1}{s_i^2} J_i(\underline{\theta}; D) \tag{3}$$

is the overall weighted measure of fit between measured and model predicted responses for all measurement locations,

$$J_i(\underline{\theta}; D) = \frac{1}{N} \sum_{m=1}^{N} \left(\hat{\varepsilon}^{(m)}(\underline{r}_i, \beta_i) - \varepsilon^{(m)}(\underline{r}_i, \beta_i; \underline{\theta})\right)^2 \tag{4}$$

is the measure of fit between measured and model predicted response at the i measured location, $\rho(\underline{s}) = \prod_{j=1}^{N_0} s_j^N$ is a scalar function of the prediction error parameter set $\underline{s}$, $\pi(\underline{\theta}, \underline{s})$ is the prior distribution for the parameter sets $\underline{\theta}$ and $\underline{s}$ and c_1 is a normalising constant estimated such that the PDF in equation (2) integrates to one. Assuming that $\underline{\theta}$ and $\underline{s}$ are independent prior to the collection of data, the prior distribution $\pi(\underline{\theta}, \underline{s})$ takes the form $\pi(\underline{\theta}, \underline{s}) = \pi_\theta(\underline{\theta}) \pi_s(\underline{s})$, where $\pi_\theta(\underline{\theta})$ and $\pi_s(\underline{s})$ are the prior distribution for the parameter sets $\underline{\theta}$ and $\underline{s}$, respectively.

Using the total probability theorem, the marginal probability distribution $p(\underline{\theta} \mid D)$ for the structural model parameters $\underline{\theta}$ is given by $p(\underline{\theta} \mid D) = \int p(\underline{\theta}, \underline{s} \mid D)\, d\underline{s}$. Substituting $p(\underline{\theta}, \underline{s} \mid D)$ from equation (2), assuming a non-informative (uniform) prior distribution $\pi_s(\underline{s})$, and carrying out analytically the integration with respect to $\underline{s}$, one obtains the exact result (Beck and Katafygiotis, 1998; Katafygiotis et al., 1998; Katafygiotis et al., 2000; Christodoulou and Papadimitriou, 2007)

$$p(\underline{\theta} \mid D) = c_2 \prod_{i=1}^{N_0} \left[J_i(\underline{\theta}; D)\right]^{-0.5(N-1)} \pi_\theta(\underline{\theta}) \tag{5}$$

where c_2 is a normalising constant ensuring that the PDF in equation (5) integrates to one. The updated PDF $p(\underline{\theta} \mid D)$ describes completely the uncertainty in the parameter set $\underline{\theta}$ given the data. In the next section, the updated PDF will be used for designing the optimal sensor configuration. The optimal value $\hat{\underline{\theta}}_{opt}$ of the parameter set $\underline{\theta}$ is obtained by maximising $p(\underline{\theta} \mid D)$ in equation (5). Equivalently, using equation (5), and assuming a uniform prior distribution for $\underline{\theta}$, the optimal value $\hat{\underline{\theta}}_{opt}$ is given by:

$$\hat{\underline{\theta}}_{opt} = \arg\min_{N_0} I(\underline{\theta}; D) \tag{6}$$

where $I(\underline{\theta};D)$ is given by:

$$I(\underline{\theta};D)=\sum_{i=1}^{N_0}\ln J_i(\underline{\theta};D). \tag{7}$$

In the special case for which $s_1 = s_2 = \ldots = s_{N_0}$, i.e. the values of the prediction error parameters are assumed to be the same, independently of the measured location, the updated PDF $p(\underline{\theta}\,|\,D)$ of the model parameters $\underline{\theta}$ takes the form as below:

$$p(\underline{\theta}\,|\,D)=c_3[J(\underline{\theta},\underline{1};D)]^{-(N_0N-1)/2} \tag{8}$$

while the optimal value $\underline{\hat{\theta}}_{opt}$ of the parameter set $\underline{\theta}$ is given by equation (6) with $I(\underline{\theta};D)$ given by:

$$I(\underline{\theta};D)=\sum_{i=1}^{N_0}J_i(\underline{\theta};D). \tag{9}$$

The crack identification problem has been formulated for the case for which only one crack exists in the region of interest. For the case of searching for multiple cracks in the region of interest, one should reformulate the problem as a model class selection problem from a family of model classes $i=1,\ldots,n_c$. The *i*th model class in the family corresponds to a model with *i* cracks in the region of interest. The Bayesian methodology for model class selection (Beck and Yuen, 2004; Papadimitriou, 2004b) can be used in this case to identify the optimal model class that fits the sensor data. This optimal model class is indicative of the number of cracks that exist in the region of interest. Bayesian methodology for parameter estimation can then be used for the optimal model class to estimate its model parameters and thus identify the locations and sizes of these cracks.

3 Optimal sensor location methodology

3.1 *Information entropy*

The updated PDF $p(\underline{\theta}\,|\,D)$ in equation (5) specifies the plausibility of each possible value of the crack parameters. It provides a spread of the uncertainty in the parameter values based on the information contained in the measured data. A unique scalar measure of the uncertainty in the estimate of the crack parameters $\underline{\theta}$ is provided by the information entropy, defined by Papadimitriou et al. (2000):

$$H(\underline{\delta},D)=E_{\theta}\left[-\ln p\left(\underline{\theta}\middle|D\right)\right]=-\int \ln p\left(\underline{\theta}\middle|D\right)\,p\left(\underline{\theta}\middle|D\right)d\theta \tag{10}$$

where $E_{\underline{\theta}}$ denotes mathematical expectation with respect to $\underline{\theta}$, and $\underline{\delta}\in R^{3N_0}$ is the sensor configuration vector, with elements the sensors' coordinates and orientations. The information entropy depends on the available data $D\equiv D(\underline{\delta})$ and the sensor configuration vector $\underline{\delta}$.

An asymptotic approximation of the information entropy, valid for large number of data ($NN_0 \to \infty$), is available (Papadimitriou, 2004a) which is useful in the experimental stage of designing an optimal sensor configuration. The asymptotic approximation is obtained by substituting equation (5) into equation (10) and observing that the resulting integral can be rewritten as Laplace-type integrals which can be approximated by applying Laplace method of asymptotic expansion (Bleistein and Handelsman, 1986). Specifically, it can be shown that for a large number of measured data, i.e. $N_0N \to \propto$, the following asymptotic results hold for the information entropy (Papadimitriou, 2004a):

$$H(\underline{\delta}, D) \sim H(\underline{\delta}; \underline{\hat{\theta}}, \underline{\hat{s}}) = \frac{1}{2} N_\theta \ln(2\pi) - \frac{1}{2} \ln[\det Q(\underline{\delta}; \underline{\hat{\theta}}, \underline{\hat{s}})] \tag{11}$$

where $\underline{\hat{\theta}} \equiv \underline{\hat{\theta}}(\underline{\delta}, D) = \arg\min_{\theta} I(\underline{\theta}; D)$ is the optimal value of the parameter set $\underline{\theta}$ that minimises the measure of fit $I(\underline{\theta}; D)$ given in equation (7), $Q(\underline{\delta}; \underline{\theta}, \underline{s})$ is an $N_\theta \times N_\theta$ positive semi-definite matrix of the form:

$$Q(\underline{\delta}; \underline{\theta}, \underline{s}) = \sum_{j=1}^{N_0} \frac{\delta_j}{s_j^2} P^{(j)}(\underline{\theta}) \tag{12}$$

known as the Fisher information matrix (Udwadia, 1994) and containing the information about the values of the crack parameters $\underline{\theta}$ based on the data from all measured positions specified in $\underline{\delta}$, while $\hat{s}_j^2$ are the optimal prediction error variances given by $\hat{s}_j^2 = J_j(\underline{\hat{\theta}})$. The matrix $P^{(j)}(\underline{\theta})$ in equation (12) is a positive semi-definite matrix given by:

$$P^{(j)}(\underline{\theta}) = \frac{1}{N} \sum_{m=1}^{N} \nabla_{\underline{\theta}} \varepsilon^{(m)}(\underline{r}_j, \beta_j; \underline{\theta})\, \nabla_{\underline{\theta}}^T \varepsilon^{(m)}(\underline{r}_j, \beta_j; \underline{\theta}) \tag{13}$$

containing the information about the values of the parameters $\underline{\theta}$ based on the data from one sensor placed at the location $\underline{r}_j$ and having orientation β_j, where $\nabla_{\underline{\theta}} = \left[\frac{\partial}{\partial \theta_1} \cdots \frac{\partial}{\partial \theta_{N_\theta}} \right]^T$ is the usual gradient vector with respect to the parameter set $\underline{\theta}$. The matrix $P^{(j)}(\underline{\theta})$ depends only on the response of the optimal model at the measurement location *j*, while it is independent of the sensor configuration vector $\underline{\delta}$.

The computation of the gradients of the strains in equation (13) depends on the type of the model class used to predict the strains in the structure. For model classes that use analytical expressions to relate the strains with the model parameters $\underline{\theta}$, the gradients of the strains are readily computed analytically. For model classes that use finite element models to compute the strains in the structure, the gradient of the strains are based on finite difference approximations.

It should be noted that the resulting asymptotic value of the information entropy, given in equation (11), does no longer depend explicitly on the measured response data *D*. The only dependence of the information entropy on the data comes implicitly through the optimal values $\underline{\hat{\theta}} \equiv \underline{\hat{\theta}}(\underline{\delta}, D)$ and $\underline{\hat{s}}^2 = [J_1(\underline{\hat{\theta}}; D), \ldots, J_{N_0}(\underline{\hat{\theta}}; D)]$. Consequently, the information entropy is completely defined by the optimal value $\underline{\hat{\theta}}$ of the model parameters and the optimal prediction error $\underline{\hat{s}}$ expected for a set of test data.

3.2 Design of optimal sensor configuration

In damage detection techniques, the aim is to design sensor configurations such that the resulting measured data are most informative about the model parameters. Since the information entropy, introduced in equation (10) as a measure of the uncertainty in the crack parameters, gives the amount of useful information contained in the measured data, the optimal sensor configuration is selected as the one that minimises the information entropy (Papadimitriou et al., 2000). That is,

$$\underline{\delta}_{best} = \arg\min_{\delta} H(\underline{\delta}; \underline{\hat{\theta}}, \underline{\hat{s}}). \tag{14}$$

However, in the initial stage of designing the experiment, the data are not available and thus an estimate of the optimal crack parameters $\underline{\hat{\theta}}$ and $\underline{\hat{s}}$ cannot be obtained from analysis. In order to proceed with the design of the optimal sensor configuration, this estimate has either to be assumed or its uncertainty has to be accounted for. In practice, the optimal sensor configuration designs are based on user-selected nominal values of the optimal model parameters $\underline{\hat{\theta}}$ and $\underline{\hat{s}}$ that are representative of the structure under study. It is worth pointing out that, as a result of the asymptotic approximation of the information entropy, the selection of the optimal sensor configuration is based solely on a nominal model, ignoring details from the measured data that are unavailable in the initial stage of experimental design.

3.3 Prediction error variance model

An analysis of the prediction error variance $s_i^2, i = 1, \ldots, N_0$ is next presented. For the prediction error induced in equation (1), it holds that

$$n^{(m)}(\underline{r}_i, \beta_i; \underline{\theta}) = n_{\mathrm{mod}el}(\underline{r}_i, \beta_i; \underline{\theta}) + n_{meas}^{(m)}(\underline{r}_i, \beta_i; \underline{\theta}), \quad i = 1, \ldots, N_0, \quad , m = 1, \ldots, N \tag{15}$$

where $n_{\mathrm{mod}el}(\underline{r}_i, \beta_i; \underline{\theta})$ accounts for the model error and $n_{meas}^{(m)}(\underline{r}_i, \beta_i; \underline{\theta})$ accounts for the measurement error. Assuming independence between the measurement error and model error, the variance s_i^2 of the total prediction error is given in the form:

$$s_i^2 = s_{i,\mathrm{meas}}^2 + s_{i,\mathrm{model}}^2 \tag{16}$$

where $s_{i,\mathrm{meas}}^2$ is the variance of the measurement error and $s_{i,\mathrm{model}}^2$ is the variance of the model error. In order to proceed with the optimal sensor configuration design, the designer has to assume values for the individual variances in equation (16). Such assumptions may depend on the nature of the problem analysed. Most studies on optimal sensor location assume that the variance of the measurement and model errors are constant, independent of the response. However, in the crack problems considered in this study, it may be reasonable to assume that the variance of the model error is proportional to the response. In addition, the response may be extremely sensitive to very small variations of the measurement location as in the case of measuring strains close to the crack tip. Specifically, due to $1/\sqrt{r}$ variation of the strain distribution, where r is the distance from the crack tip, small variations in the sensor location, due to inaccurate sensor location, may result in extremely high variations in the response close to the crack tip. Thus, the sensitivity of the measured response to sensor location may play an important role in defining the measurement and model error. To properly account for these variations, it is reasonable to assume that the error is a function of the sensitivity of the response to variations in the sensor positions. Usually this error and the corresponding prediction error variance may be considered to be a function of the measured response or its spatial derivatives.

Adding all these errors together, one can derive the following expression for the variance of the prediction error:

$$s_i^2 = c_0^2 + c_{r_i}^2 q^2(\underline{r}_i, \beta_i; \underline{\theta}) + c^2(q) \tag{17}$$

where the first term accounts for constant errors, independent of the response, the second term accounts for prediction errors that depend on the strength $q(\underline{r}_i, \beta_i; \underline{\theta})$ of the response predicted by the model and the third term accounts for prediction errors that depend on the details of the response $q \equiv q(\underline{r}_i, \beta_i; \underline{\theta})$. Further analysis and estimation of this variance for the specific case of a single crack in a thin plate is presented in Section 5.

4 Optimisation – computational issues

4.1 Hybrid optimisation algorithm

The optimisation problems (6) and (14), related to the estimation of the crack parameters and the estimation of optimal sensor configuration, result in multiple global/local optima. Conventional gradient-based local optimisation methods are unable to handle efficiently multiple local optima and may present difficulties in estimating the global minimum. They lack reliability in dealing with the optimisation problem since convergence to the global minimum is not guaranteed. Evolutionary algorithms (Beyer, 2001) are more appropriate and effective to use in such cases. Evolutionary algorithms are random search algorithms that explore better the parameter space for detecting the neighbourhood of the global optimum. They are based on a randomly initialised population of search points in the parameter space, which by means of selection, mutation and recombination evolves towards better and better regions in the search space. Details on theoretical developments of Evolution Strategies (ES) can be found in Beyer (2001). A disadvantage of ES is their slow convergence in the neighbourhood of the global optimum since they do not exploit the gradient information. For this, a hybrid optimisation algorithm is used that exploits the advantages of evolutionary and gradient-based methods. Specifically, an ES is first used to explore the parameter space and detect the neighbourhood of global minimum. Then the method switches to a gradient-based algorithm starting with the best estimate obtained from the evolutionary algorithm and using gradient information to accelerate converge to the global optimum.

Due to the random nature of the initial population used in ES, the proposed hybrid optimisation algorithm is effective in determining multiple global minima by running the algorithm several times and storing the optimal solution of each run into an optimal set of solutions. Depending on the initial population in each run, the algorithm may converge to a different global optimum in the parameter space. As the number of runs increases, the optimal set of solutions usually contains all optima solutions for the problem.

4.2 Heuristic algorithm for optimal sensor configuration

A more systematic and computationally very efficient approach for obtaining a good sensor configuration for a fixed number of N_0 sensors is to use a Sequential Sensor Placement (SSP) algorithm as follows. The positions of N_0 sensors are computed sequentially by placing one sensor at a time in the plate, starting with a minimum number of $N_{\min}$ sensors, at a position and orientation that results in the highest reduction in information entropy. The minimum number of sensors $N_{\min}$ used is the one that corresponds to an identifiable crack parameter set. This is investigated through the determinant of the matrix Q in equation (12), since when $\det(Q) \to 0$ then the number of sensors used is not enough to create an array of sensors whose measurements will result in an identifiable model. So the positions of the first $N_{\min}$ sensors are chosen as those that give the highest reduction in the information entropy for $N_{\min}$ sensors. Given the optimal positions of the first $N_{\min}$ sensors, the position of the next sensor is chosen as the one that gives the highest reduction in the information entropy computed for $(N_{\min}+1)$ sensors with the positions of the first $N_{\min}$ sensors fixed at the optimal ones already computed in the first step. Continuing in a similar fashion, given the positions of $i-1$ $\left(i \geq N_{\min}+1 \right)$ sensors in the structure computed in the previous $i-1$ steps, the position of the next ith sensor is obtained as the one that gives the highest reduction in the information entropy for i sensors with the positions of the first $i-1$ sensors fixed at the optimal ones already obtained in the previous $i-1$ steps. This procedure is continued for up to N_0 sensors. This algorithm is referred to as the SSP algorithm and has been first introduced in Papadimitriou (2004a) to handle the discrete optimisation problem. The SSP algorithm, when applied to discrete-variable optimisation problems, was shown to give sensor configurations with corresponding information entropies that are extremely close to the minimum information entropy. Its effectiveness to continuous-variable optimisation problem arising in the present study will be investigated in the applications section.

5 Applications

The effectiveness of the proposed methodology is demonstrated using simulated strain measurements $\hat{\varepsilon}$ for the mode I crack problem of Figure 3. In particular, we consider a cracked rectangular plate with sides of length L_x and L_y, under equal biaxial far field tension $\sigma_{xx}^{\infty} = \sigma_{yy}^{\infty} = \sigma$, where the x- and y-axes of the coordinate system used are parallel to the sides of the plate (Figure 3). The through-the-thickness-crack is assumed to be straight, its size is $2a$, its centre is located at (x_0, y_0) and its orientation is defined by the angle ϕ relative to the x-axis, as shown in Figure 3.

Figure 3 Case of a crack of length $2a$ in a bounded plate subjected to uniform biaxial tension at far field

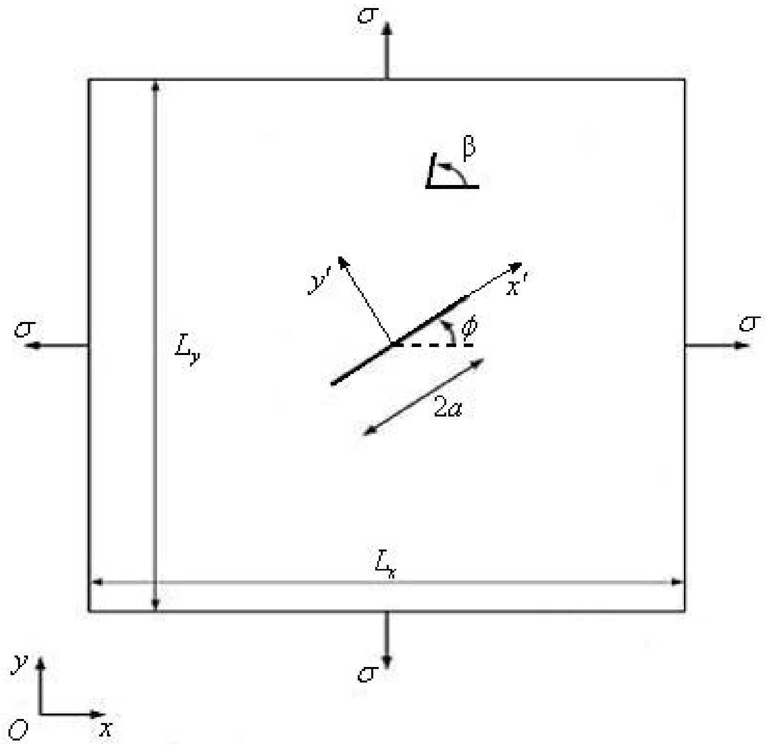

Since there are no experimental data available, simulated measured data are generated from a finite element model of the corresponding problem created with COMSOL Multiphysics (COMSOL AB) for the various crack configurations assumed and for specimen size $L_x = L_y = ea$. Zero-mean Gaussian white noise errors are added to the finite element model results in order to simulate the effect of measurement error. So the 'measured data' $\hat{\varepsilon}$ are generated as follows:

$$\hat{\varepsilon} = \varepsilon_{FEM}\left(1+\eta\right) \tag{18}$$

where ε_{FEM} are the strain values obtained from the finite element model for a given value of e, and η is a Gaussian variable with zero mean and standard deviation s.

In the results presented, the material properties are Young's modulus $E = 70\,\text{GPa}$ and Poisson ratio $v = 0.33$. In all cases examined, the simulated data were generated for these values of material properties and the following values of crack parameters: position of crack $x_0 = 0.06$, $y_0 = 0.06$, half crack length $a = 0.005$ and crack orientation $\phi = 0$. The modelled plate was subjected to uniform far field biaxial stress $\sigma = 100\,\text{MPa}$.

Model predictions of the strain field $\varepsilon(x, y)$ near and far from the crack tip are provided for various crack configurations by an analytical solution (Broek, 1984) available for this stress state and valid for an infinite plate. These predictions are accurate for practical applications, provided that the dimensions L_x and L_y are much larger than the crack length, i.e. for values of $e \gg 10$.

Specifically, the stress field for an infinite plate can be determined as below:

$$\begin{aligned}\sigma_{x'x'} &= \operatorname{Re} Z - \operatorname{Im} z \operatorname{Im} Z' \\ \sigma_{y'y'} &= \operatorname{Re} Z + \operatorname{Im} z \operatorname{Im} Z' \\ \sigma_{x'y'} &= -\operatorname{Im} z \operatorname{Re} Z'\end{aligned} \tag{19}$$

where $\sigma_{i'j'}$ are stress components relative to an (x', y') Cartesian coordinate system with origin at the centre of the crack (x_0, y_0) and with the x'- and y'-axes along and normal to the crack as shown in Figure 3, $z = x' + i\,y'$ is a complex variable, $i = \sqrt{-1}$ the imaginary unit, $Z(z)$ the Westergaard stress function defined by:

$$Z(z) = \frac{\sigma z}{\sqrt{z^2 - a^2}}, \tag{20}$$

and $Z' = dZ / dz$. For plane stress conditions, the corresponding strains are given by:

$$\begin{aligned}\varepsilon_{x'x'} &= \frac{1-\nu}{E} \operatorname{Re} Z - \frac{1+\nu}{E} \operatorname{Im} z \operatorname{Im} Z' \\ \varepsilon_{y'y'} &= \frac{1-\nu}{E} \operatorname{Re} Z + \frac{1+\nu}{E} \operatorname{Im} z \operatorname{Im} Z' \\ \varepsilon_{x'y'} &= -\frac{1+\nu}{E} \operatorname{Im} z \operatorname{Re} Z'\end{aligned} \tag{21}$$

where *E* is Young's modulus and *v* is Poisson's ratio. The strain components with respect to the original $x-y$ coordinate system are given by the well-known transformation formulae:

$$\begin{aligned}\varepsilon_{xx} &= \frac{\varepsilon_{x'x'} + \varepsilon_{y'y'}}{2} + \frac{\varepsilon_{x'x'} - \varepsilon_{y'y'}}{2} \cos 2\phi - \varepsilon_{x'y'} \sin 2\phi \\ \varepsilon_{yy} &= \frac{\varepsilon_{x'x'} + \varepsilon_{y'y'}}{2} - \frac{\varepsilon_{x'x'} - \varepsilon_{y'y'}}{2} \cos 2\phi + \varepsilon_{x'y'} \sin 2\phi \\ \varepsilon_{xy} &= \varepsilon_{x'y'} \cos 2\beta + \frac{\varepsilon_{x'x'} - \varepsilon_{y'y'}}{2} \sin 2\phi\end{aligned} \tag{22}$$

where ϕ defines the orientation of the crack relative to the *x*-axis, as shown in Figure 3. Finally, the normal strain component in the direction defined by the angle β relative to the *x*-axis (Figure 3) is determined as below:

$$\begin{aligned}\varepsilon_{\beta\beta} &= \frac{\varepsilon_{xx} + \varepsilon_{yy}}{2} + \frac{\varepsilon_{xx} - \varepsilon_{yy}}{2} \cos 2\beta + \varepsilon_{xy} \sin 2\beta = \\ &= \frac{\varepsilon_{x'x'} + \varepsilon_{y'y'}}{2} + \frac{\varepsilon_{x'x'} - \varepsilon_{y'y'}}{2} \cos 2(\phi - \beta) - \varepsilon_{x'y'} \sin 2(\phi - \beta).\end{aligned} \tag{23}$$

Also, the 'local' coordinates (x', y') are related to the 'global' coordinates (x, y) as follows:

$$
\begin{aligned}
& x' = (x - x_0)\cos\phi + (y - y_0)\sin\phi \\
& y' = -(x - x_0)\sin\phi + (y - y_0)\cos\phi \\
& \text{or} \\
& x = x_0 + x'\cos\phi - y'\sin\phi \\
& y = y_0 + x'\sin\phi + y\cos\phi.
\end{aligned} \tag{24}
$$

The two different models, the computational model used for simulating measured strain data from a bounded square plate with dimensions $L_x = L_y = L = ea$, and the analytical model used for predicting the strain field of an infinite plate structure, are purposely chosen to introduce modelling error which is always present in structural modelling. One of the purposes of the analysis is to investigate the effect of modelling error on the effectiveness of identification methodology. The size of modelling error depends on the value of the variable *e*. The smaller the value of *e*, the less accurate the analytical solution is for describing the strain field in a bounded plate, and the higher the size of modelling error.

It should be noted that the current application is based on a simple structural/crack configuration and far field stress state for which analytical results from a model are available to approximately predict the stresses/strains in the structure. In the case of structural/crack configurations or far field stress states for which analytical results are not available, the predictions of the stresses/strains throughout the structure should be based on numerical models such as finite element models. In this case, efficient computational tools need to be developed to handle the prediction of the strains in the structure using the numerical model under various crack locations, sizes and orientations. The involved computational procedures are expected to significantly increasing the computational time required for crack identification. Moreover, the gradients of the strains needed in optimising the objective function (7) or (9) and also for computing the formula (13) should be estimated in this case using finite difference approximations.

5.1 Existence of multiple local/global optima

In order to demonstrate the existence of multiple local optima, and therefore the necessity of an efficient global optimisation algorithm, we consider the case of small model error ($e = 100$), no measurement error ($\eta = 0\%$) and known far field stresses so as the parameters to be identified in this case are the crack location (x_0, y_0), half crack length a and crack orientation ϕ. Figure 4 shows the contour plots of the measure of fit in (3), as a function of the crack position x_0 and y_0, holding the values of the other parameters a and ϕ constant. A grid of 18 sensors was used to measure strains $\varepsilon_x, \varepsilon_y$ in nine locations, as shown schematically in Figure 5. It is observed from this figure that a highly nonlinear, non-convex, objective function is obtained which involves multiple local optima. It should be noted that the number of local optima depends in general on the number and locations of sensors placed in the structure. The global optimum is in the area around $x = 0.6,\quad y = 0.6$. A gradient-based optimisation method with an initial estimate chosen in one of the neighbourhoods of the local optima will fail to converge to the global optimum, leading to a sub-optimal solution corresponding to a local optimum.

Figure 4 Contour plots of the total mean-square prediction error as a function of the coordinates *x*, *y* of the crack centre (see online version for colours)

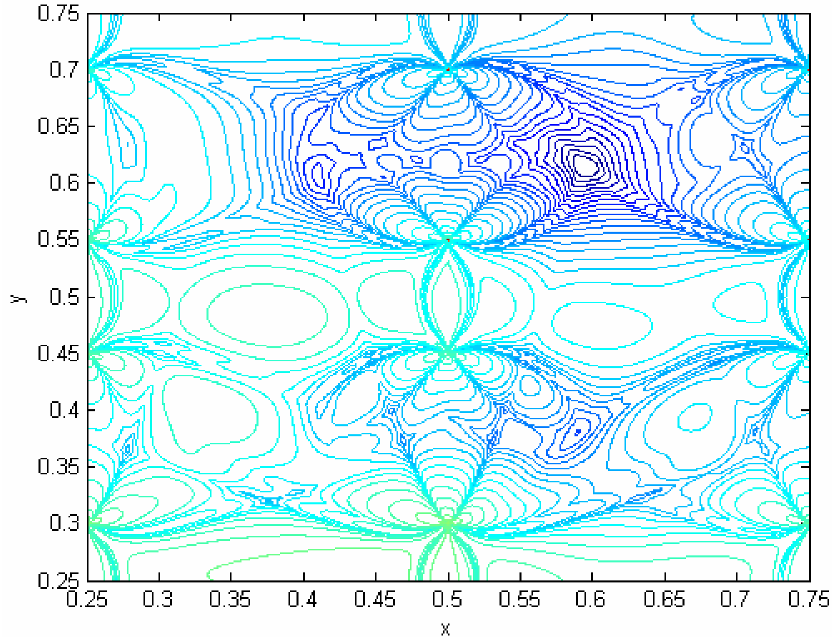

Figure 5 Crack identification using strain measurements $\varepsilon_x, \varepsilon_y$ at nine locations and considering small model error ($e = 100$) and measurement error $\eta = 2\%$

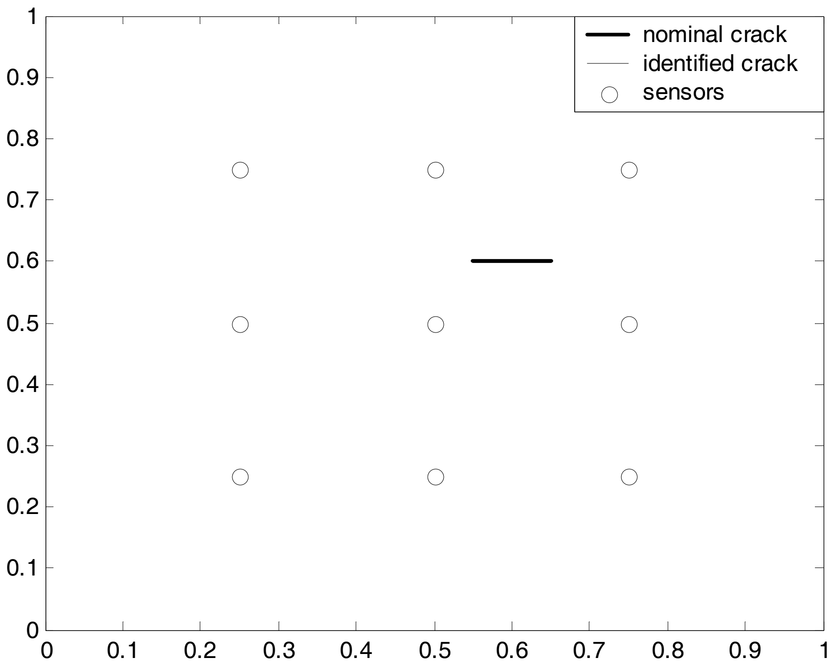

The proposed hybrid optimisation algorithm is shown to be effective in avoiding local optima and locating the global one. Evolutionary algorithms are used in these cases in order to estimate the neighbourhood of the global optimum, and then the algorithm is switched to a gradient-based optimisation algorithm that can converge quickly to the global optimum. It should be noted, however, that in order to find the neighbourhood of the global optimum, evolutionary algorithms require a relatively large number of function evaluations and this makes the proposed approach computationally time-consuming.

5.2 Sensitivity to model error

Next, the effect of model error on the effectiveness of the methodology is investigated. For this, the crack detection problem is considered for the following cases: (1) the case of plate dimensions $L = 100a$ corresponding to small model error $(e = 100)$, (2) the case of plate dimensions $L = 10a$ corresponding to medium model error $(e = 10)$ and (3) the case of plate dimensions $L = 7a$ corresponding to large model error $(e = 7)$. The respective sizes of model error are due to the fact that the analytical solutions used to predict the strain field in the identification method hold only for infinite dimensions and tend to be inaccurate as the ratio $L / a = e$ decreases. An additional $\eta = 2\%$ noise in the measurements is assumed. The crack identification results for the case $L = 100a$ were already shown in Figure 5. Results for the cases of $L = 10a$ $(e = 10)$ and $L = 7a$ $(e = 7)$ are shown in Figures 6 and 7, respectively. The optimal values of the parameter set $\underline{\theta}$ are given in Table 1 for the three cases considered. From the results in Table 1, we observe that the increase of the model error from $e = 100$ to $e = 7$ results in a certain loss of accuracy in the identified parameters. Specifically, for medium model error $(e = 10)$ there is a 7% relative error in the estimation of cracks half-length, while in the case of large model error $(e = 7)$ there is a 12% relative error in the estimation of the size of the crack combined with an error of 3% in the estimate of cracks location. Also, the orientation of the crack predicted by the methodology is slightly missed by approximately $3° - 4°$. It should be noted that the estimates deteriorate as the model error increases or, equivalently, the value of e decreases. The results in Table 1 demonstrate that the proposed methodology can efficiently detect a crack in a thin plate, and estimate with sufficient accuracy its size and orientation, as well as the unknown load to which the plate is subjected to.

5.3 Parametric analysis

The limits on which this methodology tends to or completely fails to identify the crack are examined next. These limits depend on several parameters such as the sensor configuration, the density of the sensors array with respect to the crack location and size, the measurement direction of the strain sensors, the orientation of the crack, etc. The following analysis investigates the effect of these parameters on the accuracy of the identification algorithm.

Figure 6 Crack identification using strain measurements $\varepsilon_x, \varepsilon_y$ at nine locations and considering medium model error ($e = 10$) and measurement error $\eta = 2\%$

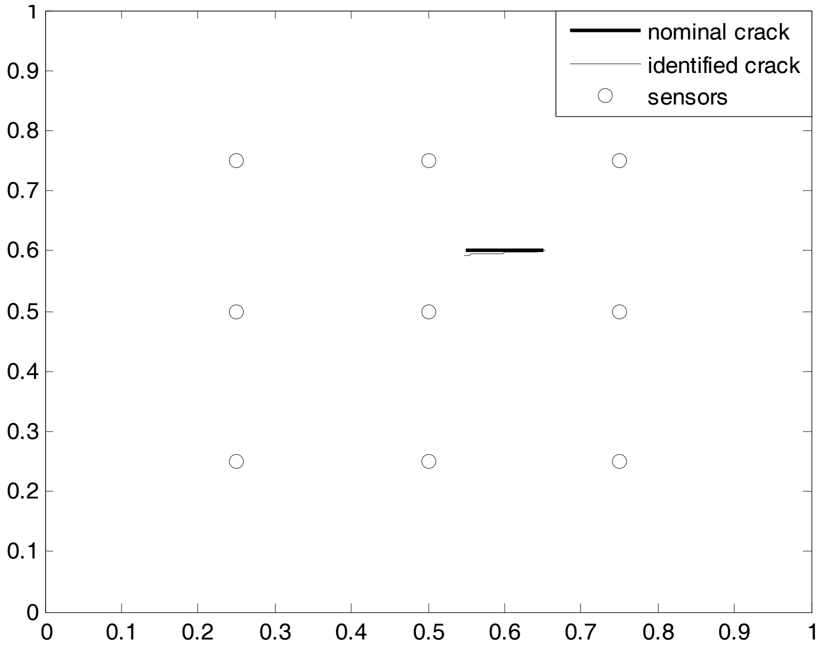

Figure 7 Crack identification using strain measurements $\varepsilon_x, \varepsilon_y$ at nine locations and considering large model error ($e = 7$) and measurement error $\eta = 2\%$

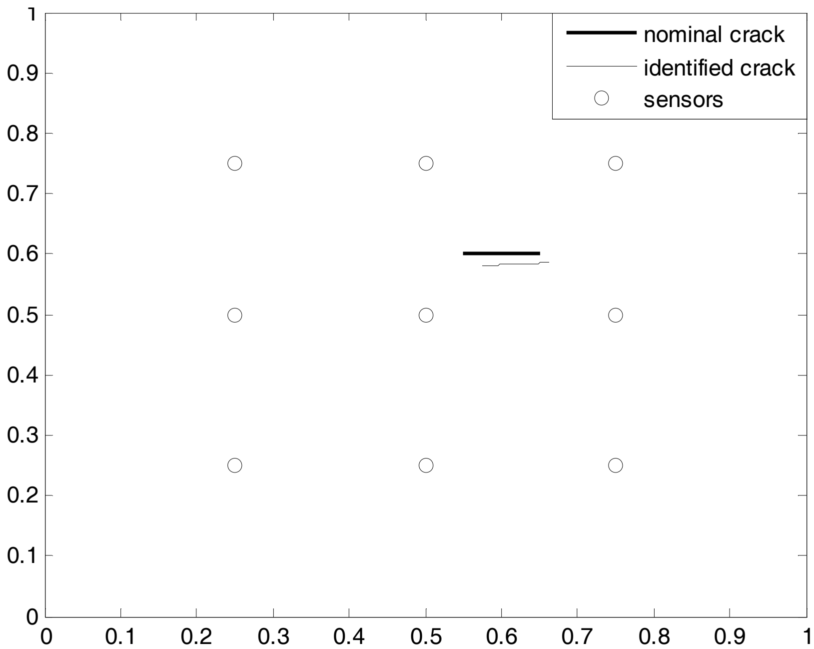

Table 1 Identification results for small, medium and large model errors corresponding to e = 100, 10 and 7, respectively

		Parameters									
		x_0		y_0		a		ϕ		σ (x100 MPa)	
Model error (e)	*Measurement error (%)*	*Nominal value (n.v.)*	*Prediction (pr.)*	*n.v.*	*pr.*	*n.v.*	*pr.*	*n.v.*	*pr.*	*n.v.*	*pr.*
100	2	0.06	0.0606	0.06	0.0597	0.005	0.00517	0°	0.05°	1.0	0.996
10	2	0.06	0.05966	0.06	0.05964	0.005	0.00536	0°	3.75°	1.0	0.9885
7	2	0.06	0.0618	0.06	0.0583	0.005	0.00438	0°	3.1°	1.0	1.0004

First, let γ be the distance of the sensor locations in the 3×3 uniform grid of sensors measuring ε_x and ε_y, shown in Figure 8. We introduce the parameter $p_1=\gamma/a$, where a is the half crack length, and examine the relative errors in the estimation of crack parameters for different values of p_1.

Figure 8 Geometric representation of sensor locations with respect to crack ($\gamma=$ distance between sensors, x_c = distance from crack to centre sensor, a = half crack length and $\beta=$ measurement direction of strain sensor)

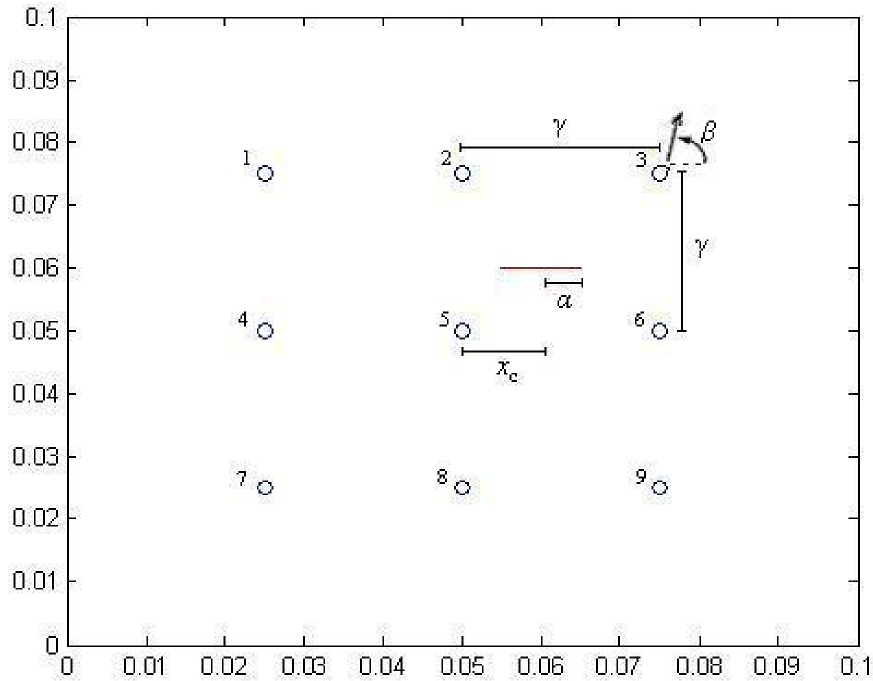

In all results shown next, we consider the case of small model error $e=100$ and measurement error $\eta=2\%$. The far field uniform stress σ is considered to be unknown and it is part of the parameter set $\underline{\theta}$ to be identified from the methodology.

In Figure 9, the relative error in the estimation of the cracks location and size for larger values of p_1 is presented. For $p_1<5$, values not shown in Figure 9, the methodology identifies accurately all crack parameters. It is observed that for $p_1=10$ the methodology has failed to detect the crack since the relative error in the coordinates estimation reaches a value of 50% in addition to a 13% relative error in determining the half crack length. It must be noted here that even in this case, the crack orientation ϕ and the far field stresses σ, not shown in Figure 7, were accurately estimated.

Figure 9 Relative errors in the estimation of x_0, y_0 and a as a function of p_1 (see online version for colours)

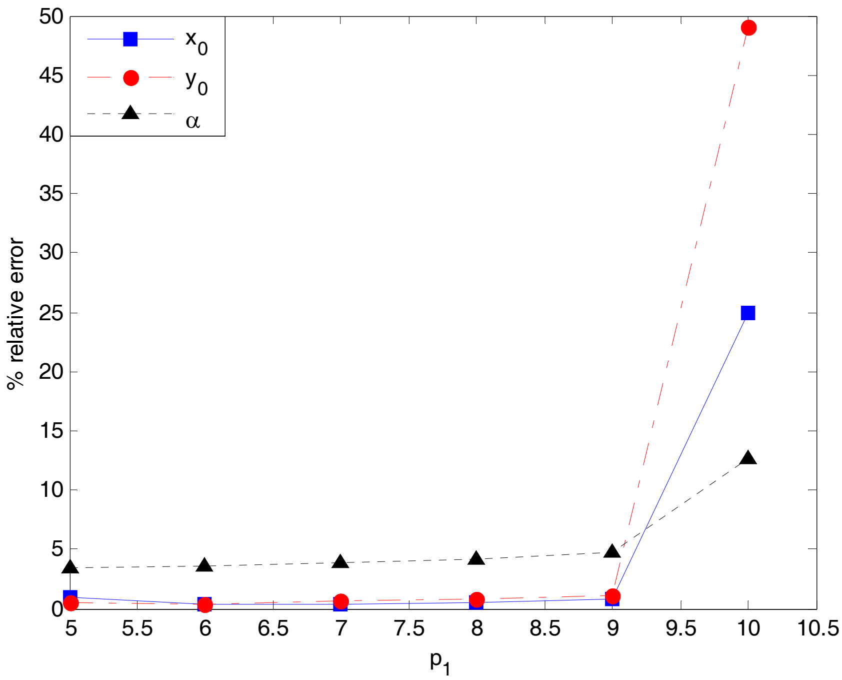

Of great importance is also the method's dependence on the crack location and especially its distance from the central sensor with respect to the cracks size. For this reason, we consider the parameter $p_2 = x_c / \alpha$, where x_c is the distance of the crack centre from the central sensor along the *x*-axis, as shown in Figure 8. Values of the relative errors in the estimated values of cracks location coordinates x_0, y_0 and half crack length a are presented in Figure 10 for value of the ratio $p_1 = \gamma / a = 5$. It is observed that as the crack moves far from the central sensor, errors in the crack location estimation slightly increase while there is a larger error of about 9% in the estimated half crack length. For larger p_1 values, these errors tend to increase. For $p_2 \geq 4$, the crack approaches the sensors 5 and 6 and these errors decrease with the accuracy of the methodology to improve significantly.

In all results presented before, an array of sensors measuring strains in *x*, *y* direction was used, while the crack had an orientation $\phi = 0°$. This means that strain measurements were obtained simultaneously in parallel and perpendicular directions with respect to the cracks orientation. We examine next the case where nine instead of 18 sensors are used to measure strains in a direction β, while the crack has an orientation $\phi = 0$, as shown in Figure 8. Two cases are examined corresponding to values $\beta = 0$ and $\beta = \pi / 2$. The value of $\beta = 0$ corresponds to the case where the strain measurements are parallel to the crack, while the value of $\beta = \pi / 2$ corresponds to strain measurements perpendicular to the crack. Identification results are examined as a function of p_1. A comparison of the relative errors on the estimation of cracks location coordinates x_0 and y_0 for the two values of the parameter β is presented in Figure 11. It is clear that when measuring strains in a direction parallel to the crack, the methodology fails to estimate crack parameters for smaller values of the ratio $p_1 = \gamma / \alpha$ than the case of strains obtained perpendicular to the crack. This conclusion will be reinforced by the results of the optimal sensor location methodology shown next, where for the crack orientation $\phi = 0°$ the methodology results in an optimum measurement direction $\beta = \pi / 2$ or $3\pi / 2$ for all sensors.

Figure 10 Relative errors in the estimation of x_0, y_0 and a as a function of p_2 (see online version for colours)

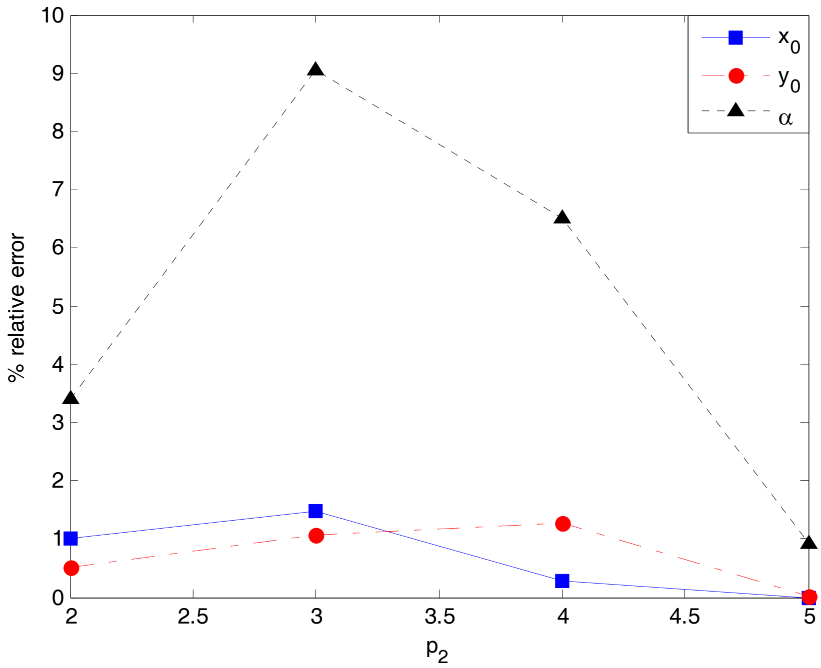

5.4 Optimal sensor configurations

Next we estimate the optimal sensor configuration for a given number of sensors using the theoretical analysis presented in Section 3. Two cases A and B are considered. In Case A, the variables to be estimated are the locations of strain sensors measuring ε_x and ε_y in a measurement location, so the search of the optimal sensor configuration for n sensors corresponds to $n / 2$ optimal locations. In Case B, one sensor is placed at each location measuring the strain at a direction β. Thus, the variables to be estimated in the search of the optimal configuration include the location and the direction of measurements as well. In this case, the sensor configuration vector $\underline{\delta} \in R^{3N_0}$ includes not only coordinates of each sensor, but angles β of measurement direction as well.

Figure 11 Relative errors in the estimation of x_0 for $p_3 = \pi/2$ and $p_3 = 0$ as a function of p_1 (see online version for colours)

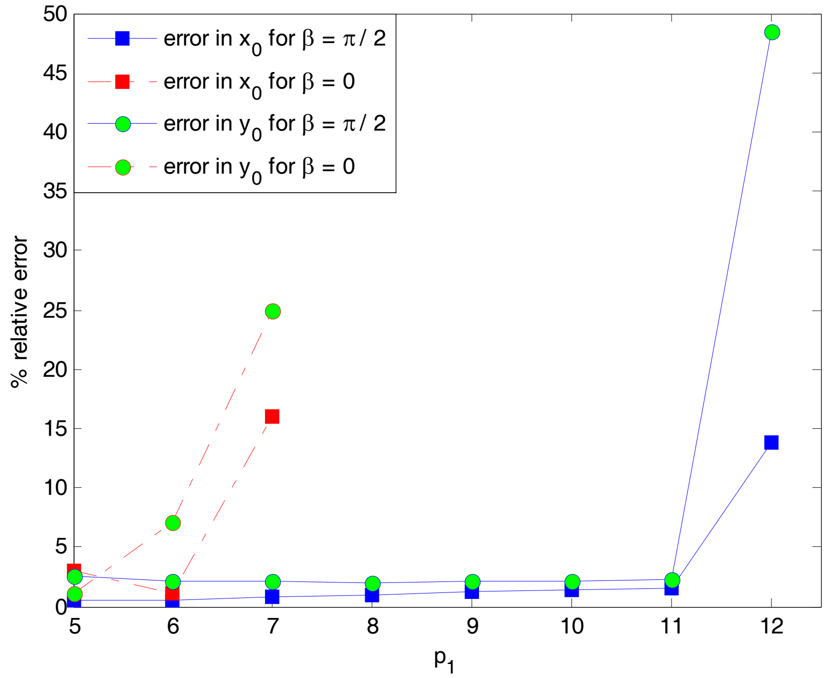

5.4.1 *Selection of the prediction error*

The estimation of the optimal sensor configuration depends on the selection of the prediction error parameters involved in the prediction error equation (17). In all results presented here, the value of the prediction error variance s_i^2 is chosen as follows.

First we will define the third term in prediction error equation (17) that depends on the nature of the response. For the strain ε near the crack tip, it holds

$$\varepsilon \sim \frac{a}{\sqrt{r}} = \frac{a(K_I, E, v)}{\sqrt{r}} \tag{25}$$

where r is the distance from the crack tip, K_I is the stress intensity factor, E is Young's modulus and v is Poisson's ratio. Due to the $1/\sqrt{r}$ variation of the strain distribution, small variations in the sensor location may result in extremely high variations in the response close to the crack tip. To properly account for these extreme variations, it is reasonable to assume that the error is a function of the response's spatial derivatives with respect to r. Considering an inaccurate sensor placement of about Δr, using equation (25), and selecting the standard deviation of the error to be proportional to the local change $\Delta\varepsilon$ of the strain, the measurement error's standard deviation is as below:

$$s_{meas} \sim \Delta\varepsilon \approx \frac{d\varepsilon}{dr}\cdot\Delta r = \frac{d}{dr}\left(\frac{a}{\sqrt{r}}\right)\cdot\Delta r = -\frac{a}{2r\sqrt{r}}\cdot\Delta r. \tag{26}$$

Substituting (26) into the general form of the measurement error's variance equation (17) and neglecting the first term (constant errors), the model prediction error variance is given by:

$$s_r^2 = s_{\text{model}}^2\cdot\varepsilon_r^2 + \left(\frac{a}{2\cdot r\cdot\sqrt{r}}\right)^2\cdot\Delta r^2 \tag{27}$$

where s_{model} and Δr are user-selected values.

Near the crack tip ($r \to 0$), the second term in equation (27) dominates the overall prediction error variance, while far from the crack tip it is the first term in equation (27) that dominates the prediction error variance. The extent of these regions of domination depend on the value of the ratios $s_{\text{model}}/\Delta r$. Herein, in all results presented, this ratio is selected, for demonstration purposes, to be $s_{\text{model}}/\Delta r = 0.5$.

5.4.2 Results of optimal sensor locations and information entropy for Case A

First, the Case A is considered with two strain sensors at an optimal location measuring strains ε_x and ε_y. A comparison between two different optimal sensor configurations using six sensors is made in Figure 12. The first one (red cross) corresponds to sensors providing information about the crack parameter set $\underline{\theta} = \{x_0, y_0, a, \phi\}$, while the other one (blue cross) corresponds to sensors providing information about the crack parameter set $\underline{\theta} = \{x_0, y_0, a, \phi, \sigma\}$ including the unknown far field stress σ as well. As expected, the sensor configuration that provides information about the additional unknown far field stress parameter contains sensors that are located in relatively larger distance from the crack tip.

In all results shown next, the optimal sensor configurations correspond to sensors providing information about the crack parameters set $\underline{\theta} = \{x_0, y_0, a, \phi, \sigma\}$. The optimal sensor configurations for Case A are illustrated in Figures 13 (a–d) for 6, 8, 10 and 12 sensors, respectively. These configurations were estimated using the hybrid optimisation algorithm for optimising the information entropy. Comparing the two different optimal sensor locations shown in Figures 12 and 13(a) for six sensors, it can be clearly seen that there are more than one global solution to the optimal sensor configuration problem that are symmetric with respect to the central axis perpendicular to the crack. The application of the hybrid optimisation algorithm converges to one of the global solutions. Repeating applications of the hybrid optimisation algorithm will eventually result in the estimation of all global solutions that exist due to the symmetry of the problem. Thus, it should be noted that the results shown in Figures 13 (a–d) for 6, 8, 10 and 12 sensors correspond to one of the multiple global solutions existing due to symmetry.

Figure 12 Comparison of optimal sensor locations providing information about the crack parameter set $\underline{\theta} = \{x_0, y_0, a, \phi\}$ (red cross) and $\underline{\theta} = \{x_0, y_0, a, \phi, \sigma\}$ (blue cross) (see online version for colours)

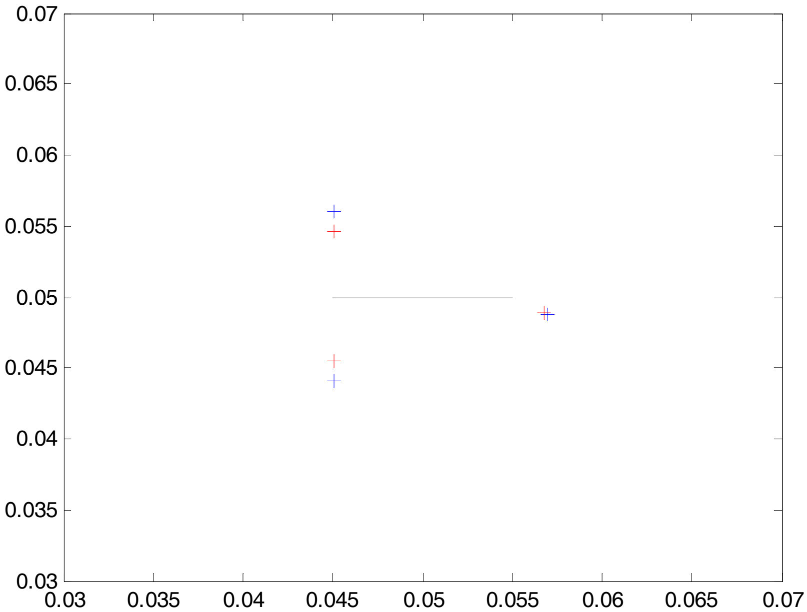

Figure 13 Optimal sensor locations for (a) 6, (b) 8, (c) 10 and (d) 12 sensors (see online version for colours)

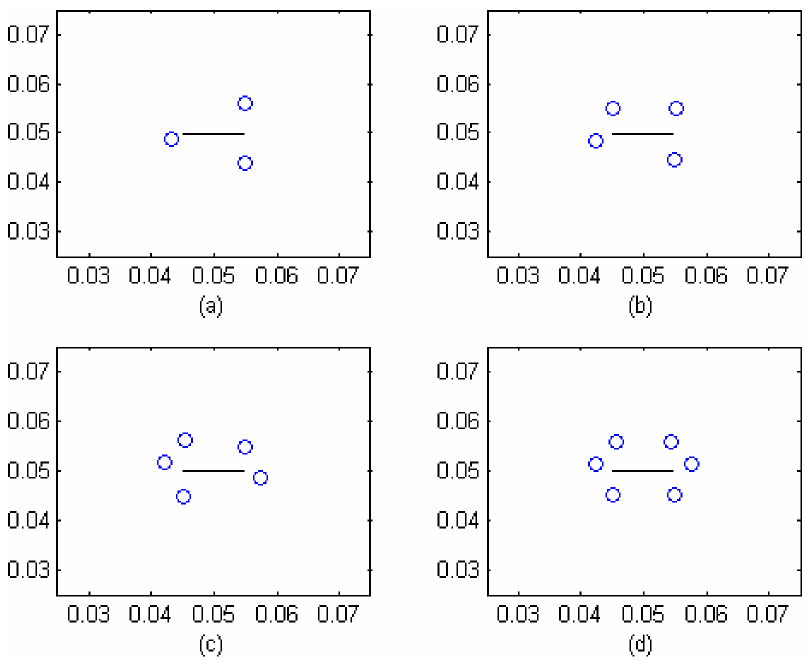

The SSP algorithm also provides optimal sensor configurations with a minimum computational effort and little loss of information. A comparison between the information entropy of the optimum configurations estimated with the hybrid optimisation algorithm and the corresponding ones estimated with the SSP algorithm is shown in Figure 14. The estimates from the direct exact algorithm and the approximate SSP algorithm are very close, validating the very good accuracy of the SSP algorithm.

Figure 14 Minimum information entropy vs. the number of sensors for the cases of hybrid optimisation and SSP algorithm (see online version for colours)

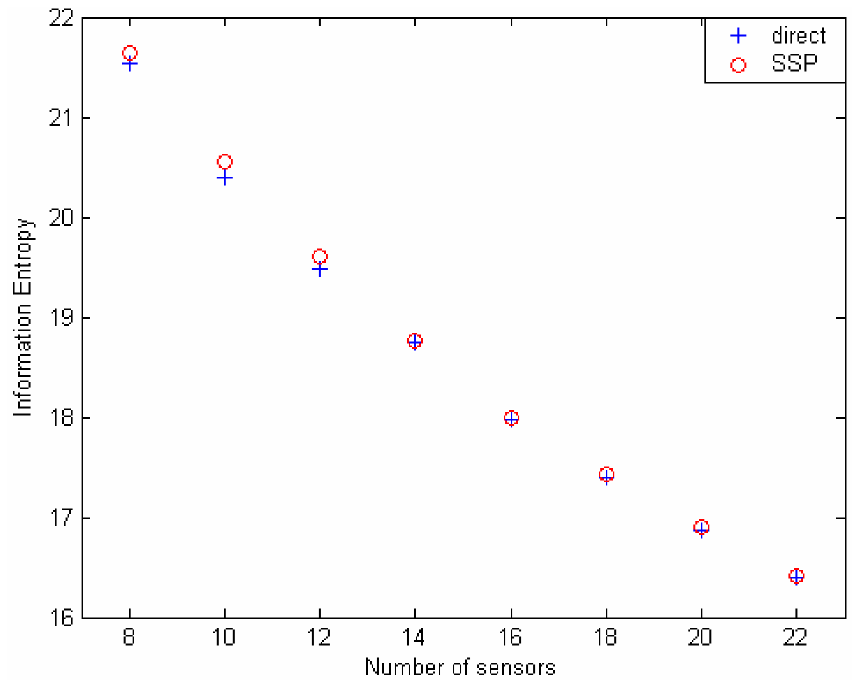

5.4.2.1 Existence of multiple global/local optima

Consider again the estimation of the optimal sensor location of 12 sensors measuring in ε_x and ε_y directions. Let the five optimal locations to be known using the direct hybrid optimisation method. The SSP algorithm is used to find the sixth location for the 11th and the 12th sensor. The contour plots of the information entropy as a function of the coordinates *x* and *y* of the sensor location is illustrated in Figure 15. It is seen that at least eight local optima exist. The sixth global optimal location found with the SSP method is shown with the cross. It is clear that the optimisation method for estimating the sixth optimal sensor location should be able to identify the global optimum from the total of eight global/local ones. Thus, the proposed hybrid optimisation algorithm is required to be used since it can locate global optima in the expense of high computational effort. It is worth pointing out that even with the SSP algorithm, the use of the hybrid optimisation is necessary. This increases significantly the computational time for estimating the optimal sensor configurations.

Figure 15 Contour plots of the information entropy as a function of the sensor location coordinates x_6 and y_6 (see online version for colours)

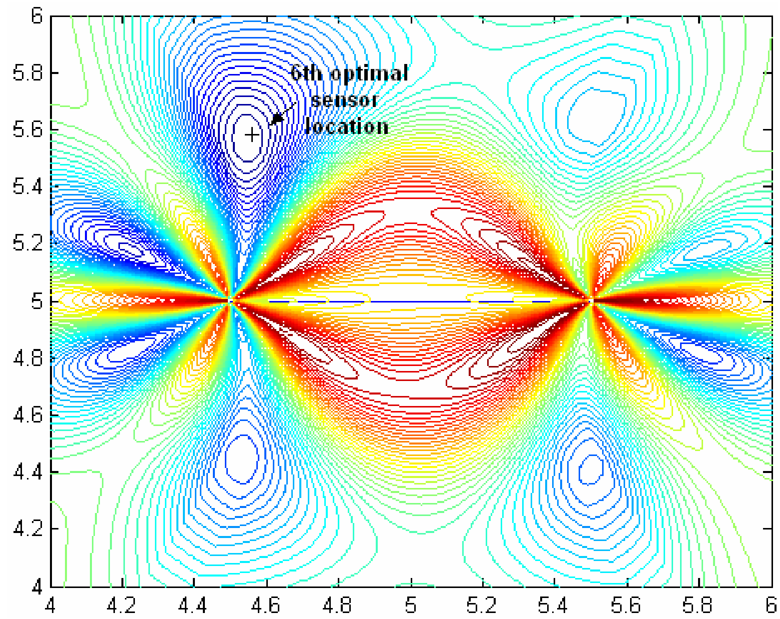

5.4.2.2 *Uncertainty in crack parameter estimates*

Consider the case of an optimal sensor configuration of 12 sensors for Case A and a corresponding arbitrary grid, as shown in Figure 16. The arbitrary grid is chosen purposely to be closest to the crack. Crack identification results are carried out with these two sensor configurations and the probability distribution $p(\underline{\theta} \mid D)$ of the crack parameters is obtained. Simulated data were generated from a finite element model of a plate with dimension $L = 100a$ and measurement error $n = 2\%$ was added to the computed strains. Figures 17 and 18 show the contour plots of the probability distribution $p(\underline{\theta} \mid D) / c_1 \pi_\theta(\underline{\theta})$ of the parameter set $\underline{\theta}$ as a function of the crack parameters x_0 and a, holding the rest of the crack parameters y_0, ϕ and stress σ constant. The global optimum is in the area around $x_0 = 0.5$, $a = 0.05$ and corresponds to the chosen values of these parameters in the finite element model that generated the measured data $\hat{\varepsilon}$.

The probability distribution in Figure 17 corresponds to the optimal sensor configuration, while the probability distribution in Figure 18 corresponds to the arbitrary grid of sensors used. It is observed from these figures that in spite of the grid of sensors chosen to be closest to the crack, the use of an optimal sensor configuration resulted in a narrower distribution, especially in the direction of x_0, compared to the much wider distribution obtained from the arbitrary grid. This demonstrates that the uncertainty in the parameter values, quantified by $p(\underline{\theta} \mid D)$, is less for the optimal configuration than it is for an arbitrary grid of sensors. Consequently, the data obtained from the optimal sensor configuration contain more information for identifying the model parameters than the data obtained from the arbitrary grid of sensors.

Figure 16 Optimal and arbitrary sensor configurations for the case of 12 sensors (see online version for colours)

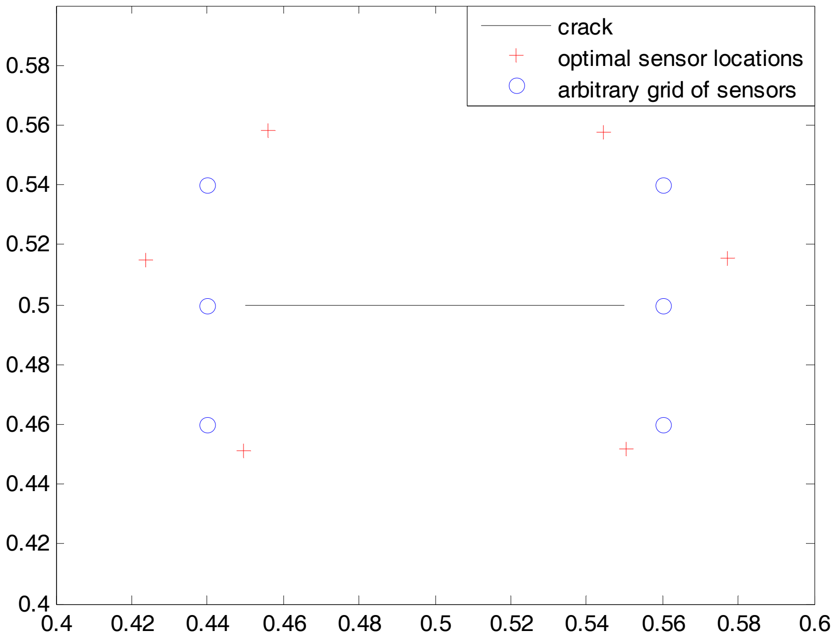

Figure 17 (a) Contour plots of probability distribution as a function of the crack centre x_0 and the crack's half-length a, and (b) zoom in the neighbourhood of the optimum, for the case of optimal sensor configuration (see online version for colours)

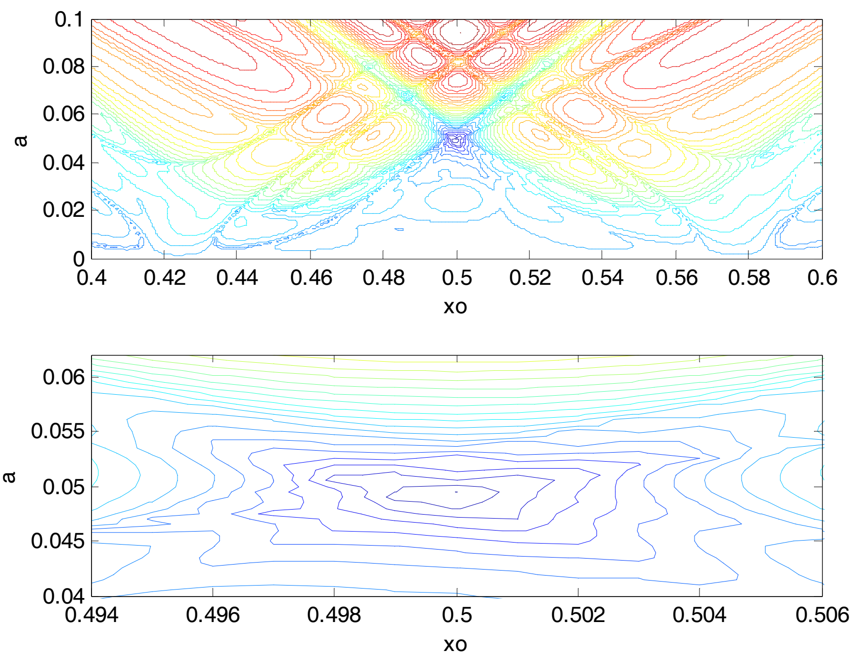

Figure 18 (a) Contour plots of probability distribution as a function of crack centre x_0 and the crack's half-length a and (b) zoom in the neighbourhood of the optimum, for the case of an arbitrary grid of sensors (see online version for colours)

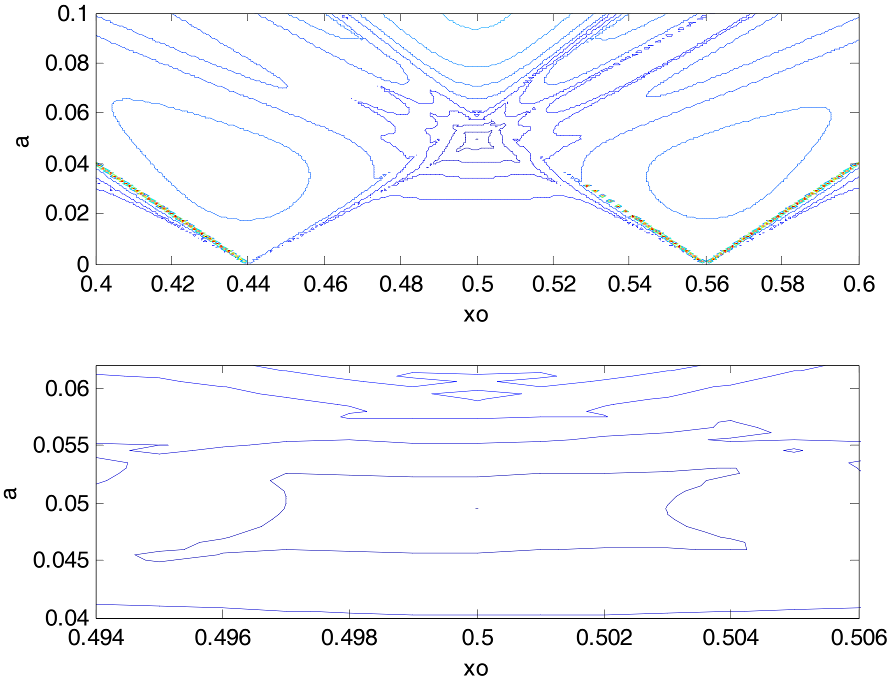

5.4.3 Results of optimal sensor configuration and information entropy for Case B

Next, results for the Case B are obtained. The optimal sensor configurations for 6, 8, 10 and 12 sensors are illustrated in Figures 19 (a–d). In this case, the direction in which sensors are placed to measure strains is not prespecified. Instead, it is considered as a variable to be optimised. For this case where the direction β of strain measurements is optimised, the problem of finding the global optima for both sensor location and the measurement angle becomes computationally more difficult. Results showed that the optimal angle of measurement for all sensors is $\beta = \pi / 2$ or $3\pi / 2$.

The minimum values of the information entropy as a function of the number of sensors placed at the optimal location in the structure are compared in Figure 20 for Cases A and B. In case B, all sensors placed at optimal locations measure strains in optimal direction that corresponds to $\beta = \pi / 2$ or $3\pi / 2$. Case B results in configurations with less information entropy, i.e. providing more informative data than in Case A, for the same number of sensors used in both cases A and B.

Figure 19 Optimal sensor locations for (a) five, (b) six, (c) seven and (d) eight sensors. Optimal measurement direction $\beta = \pi/2$ or $3\pi/2$ for all sensors (see online version for colours)

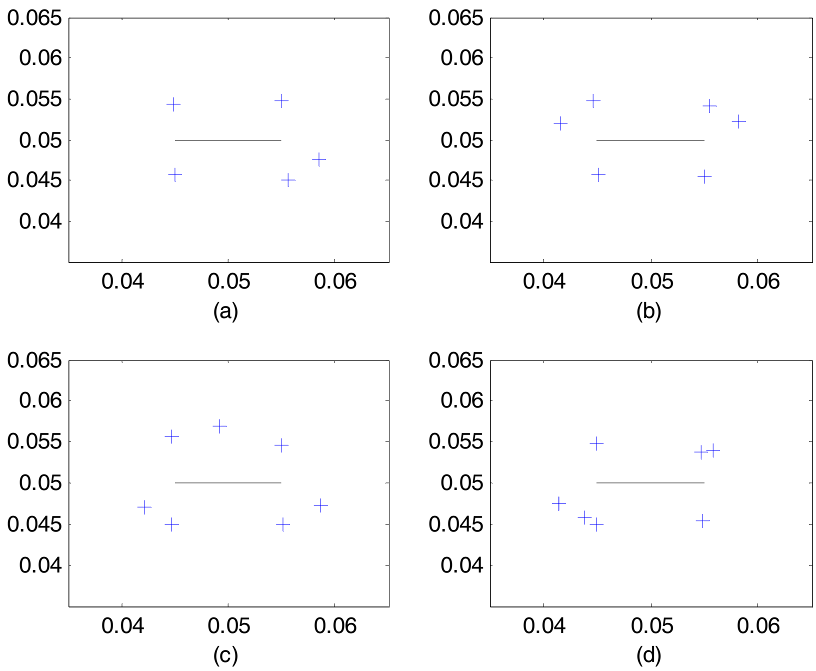

Figure 20 Minimum information entropy vs. the number of sensors for cases A (red) and B (blue) (see online version for colours)

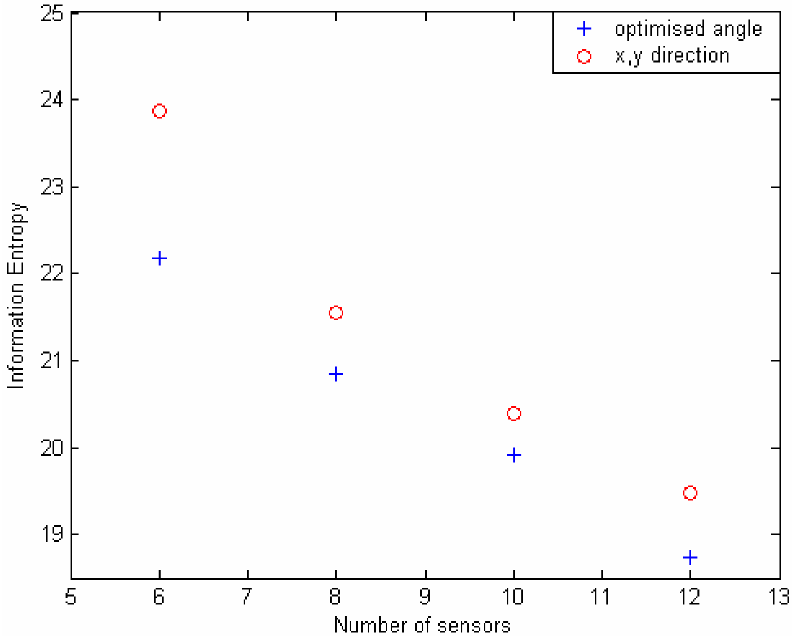

6 Conclusions

A methodology was presented for the estimation of cracks in structures using strain measurements. A Bayesian system identification methodology was used to estimate the location, size and orientation of cracks using the information provided from strain measurements of a cracked thin plate subjected to uniform stress. The analysis showed that the proposed identification methodology can efficiently detect and completely identify an existing crack and far field stresses using a simple grid of sensors, even in the presence of measurement and model errors, provided that these model errors are sufficiently small.

A parametric analysis was performed with variables: (1) the density of the sensor configuration with respect to the crack size, (2) the distance of cracks centre from the central sensor of a uniform 3 × 3 grid of strain sensors with respect to the crack size and (3) the difference between the crack orientation and the direction of the strain measurements. This analysis provided useful insight about the effect of these variables to the method's accuracy, as well as the limits on which this methodology fails to identify the crack. Results showed that for $\gamma / a < 10$, where γ is characteristic of the sensor grid and a is the half crack length, the methodology can completely identify a crack and the external static load for both cases of strain measurements ε_x, ε_y in each sensor location and that of strain measurements perpendicular to the crack. For the case of strain measurements in a direction parallel to the crack, the values of γ / a for estimating the crack parameters are significantly smaller.

Optimal sensor configurations using the information entropy measure were also derived. A comparison between the case of optimal sensor configurations using sensors measuring strains ε_x and ε_y in an optimal location and the case of configurations with sensors placed at optimal locations measuring strains in an optimal direction β was made. The latter case resulted in configurations that provided more informative data for the same number of sensors than the first case. Results also showed that the optimal measurement direction for all strain sensors is $\pi / 2$ or $3\pi / 2$ with respect to the crack orientation. This means that most of the information about the crack parameters is derived by strain measurements in a perpendicular direction with respect to the crack, a result also reinforced by the parametric analysis results.

Both optimisation problems involved in crack identification and optimal sensor configuration methodologies were proven to have multiple local and global optima. Thus, the use of an effective optimisation algorithm is necessary. Evolutionary algorithms are used in order to estimate the neighbourhood of the global optimum, and then the algorithm is switched to a gradient-based optimisation algorithm that can converge quickly to the global optimum. The proposed hybrid optimisation algorithm is shown to be effective in avoiding local optima and locating the global one. However, in order to find the neighbourhood of the global optimum, evolutionary algorithms require a relatively large number of function evaluations and this makes the proposed approach computationally time-consuming.

Despite the computational effort needed and the limitations as far as model and measurement errors are considered, the proposed identification methodology was proven to be able to detect a crack in a thin plate subject to far field static load, as well as to accurately identify the crack size and orientation.

Acknowledgements

This research was co-funded 75% from the European Union (European Social Fund), 25% from the Greek Ministry of Development (General Secretariat of Research and Technology) and from the private sector, in the context of measure 8.3 of the Operational Programme Competitiveness (3rd Community Support Framework Programme) under grant 03-ΕΔ-524 (PENED 2003).

References

Beck, J.L. and Katafygiotis, L.S. (1998) 'Updating models and their uncertainties-Bayesian statistical framework', *Journal of Engineering Mechanics (ASCE)*, Vol. 124, No. 4, pp.455–461.

Beck, J.L. and Yuen, K.V. (2004) 'Model selection using response measurements: Bayesian probabilistic approach', *Journal of Engineering Mechanics (ASCE)*, Vol. 130, No. 2, pp.192–203.

Beyer, H.G. (2001) *The Theory of Evolution Strategies*, Springer, Berlin.

Bleistein, N. and Handelsman, R. (1986) *Asymptotic Expansions for Integrals*, Dover, New York, USA.

Broek, D. (1984) *Elementary Engineering Fracture Mechanics*, Martinus Nijhoff, The Hague.

Christodoulou, K. and Papadimitriou, C. (2007) 'Structural identification based on optimally weighted modal residuals', *Mechanical Systems and Signal Processing*, Vol. 21, No. 1, pp.4–23.

COMSOL AB (2005) *Comsol Multiphysics User's Guide*. Available online at: http://www.comsol.com/

Doebling, S.W., Farrar, C.R. and Prime, M.B. (1998) 'A summary review of vibration-based damage identification methods', *The Shock and Vibration Digest*, Vol. 30, No. 2, pp.91–105.

Doebling, S.W., Farrar, C.R., Prime, M.B. and Shevitz, D.W. (1996) *Damage Identification and Health Monitoring of Structural and Mechanical Systems from Changes in their Vibration Characteristics: A Literature Review*, Los Alamos National Laboratory, Report No. LA-13070-MS.

Giurgiutiou, V., Bao, J. and Zhao, W. (2001) 'Active sensor wave propagation health monitoring of beam and plate structures', *Proceedings of the SPIE's 8th International Symposium on Smart Structures and Materials*, 4–8 March, Newport Beach, CA.

Hjelmstad, K.D. and Shin, S. (1996) 'Crack identification in a cantilever beam from modal response', *Journal of Sound and Vibration*, Vol. 198, pp.527–545.

Ihn, J.B. and Chang, F.K. (2004) 'Detection and monitoring of hidden fatigue crack growth using a built-in piezoelectric sensor/actuator network: part I. Diagnostics', *Smart Materials and Structures*, Vol. 13, pp.609–620.

Kammer, D.C. (1991) 'Sensor placements for on orbit modal identification and correlation of large space structures', *Journal of Guidance, Control and Dynamics*, Vol. 14, pp.251–259.

Katafygiotis, L.S., Lam, H.F. and Papadimitriou, C. (2000) 'Treatment of unidentifiability in structural model updating', *Advances in Structural Engineering – An International Journal*, Vol. 3, No. 1, pp.19–39.

Katafygiotis, L.S., Papadimitriou, C. and Lam, H.F. (1998) 'A probabilistic approach to structural model updating', *International Journal of Soil Dynamics and Earthquake Engineering*, Vol. 17, Nos. 7–8, pp.495–507.

Kirkegaard, P.H. and Brincker, R. (1994) 'On the optimal locations of sensors for parametric identification of linear structural systems', *Mechanical Systems and Signal Processing*, Vol. 8, pp.639–647.

Lee, B.C. and Staszewski, W.J. (2003) 'Modeling of Lamb waves for damage detection in metallic structures: part II. Wave interactions with damage', *Smart Materials and Structures*, Vol. 12, pp.815–824.

Mal, A.K., Ricci, F., Banerjee, S. and Shih, F.A. (2005) 'Conceptual structural health monitoring system based on vibration and wave propagation', *Structural Health Monitoring: An International Journal*, Vol. 4, No. 3, pp.283–293.

Munns, T.E., Bartolini, A., Kent, R.M. and Bartolini, A. (2002) 'Health monitoring for airframe structural characterization', NASA/CR-2002-211428, NASA Langley Research Center, Hampton, Virginia.

Paget, C., Grondel, S., Levin, K. and Delebarre, C. (2003) 'Damage assessment in composites by Lamb waves and wavelet coefficients', *Smart Materials and Structures*, Vol. 12, pp.393–402.

Papadimitriou, C. (2004a) 'Optimal sensor placement methodology for parametric identification of structural systems', *Journal of Sound and Vibration*, Vol. 278, No. 4, pp.923–947.

Papadimitriou, C. (2004b) 'Bayesian inference applied to structural model updating and damage detection', *9th ASCE Joint Specialty Conference on Probabilistic Mechanics and Structural Reliability*, Albuquerque, New Mexico.

Papadimitriou, C., Beck, J.L. and Au, S.K. (2000) 'Entropy-based optimal sensor location for structural model updating', *Journal of Vibration and Control*, Vol. 6, No. 5, pp.781–800.

Tsamasphyros, G.J., Furnarakis, N., Kanderakis, G. and Marioli-Riga, Z. (2003a) 'Optimization of embedded optical sensor location in composite repairs', *Applied Composite Materials*, Vol. 10, pp.129–140.

Tsamasphyros, G.J., Kanderakis, G.N., Furnarakis, N.K., Marioli-Riga, Z.P., Chemama, R. and Bartolo, R. (2003b) 'Selection of optical fibers paths and sensor locations for monitoring the integrity of composite patching', *Applied Composite Materials*, Vol. 10, pp.331–338.

Udwadia, F.E. (1994) 'Methodology for optimal sensor locations for parameter identification in dynamic systems', *Journal of Engineering Mechanics (ASCE)*, Vol. 120, No. 2, pp.368–390.

Vanik, M.W., Beck, J.L. and Au, S.K. (2000) 'Bayesian probabilistic approach to structural health monitoring', *Journal of Engineering Mechanics (ACSE)*, Vol. 126, pp.738–745.